

Investigation of an Innovative Latent Heat Storage Concept in a Stovepipe

Alexis Sevault^{*a}, Jerol Soibam^b, Nils Erland L. Haugen^{a,b}, Øyvind Skreiberg^a

^aSINTEF Energy Research, P.O.Box 4761 Torgarden, NO-7465 Trondheim, Norway

^bNTNU - Norwegian University of Science and Technology, Energy and Process Engineering, 7491 Trondheim, Norway

*Alexis.Sevault@sintef.no

Latent heat storage (LHS) is a promising concept for small-scale batch combustion. One example is wood stoves, which rely on a batch combustion process that yields a transient heat production with high peak effect. A well-designed LHS system with phase change material (PCM), with melting temperature in the range of 100-150 °C, can flatten out the peak heat effects and release the heat to the room over an extended time-period. The objective of the current study was to design a compact and durable LHS system capable of storing a substantial part of the heat produced during the combustion phase and to effectively release the stored heat to the room for 6 to 10 hours after the combustion phase ends. A passive LHS system designed as a coaxial cylinder acting as a stovepipe located at the top of a wood stove was simulated by utilizing a transient two-dimensional axisymmetric approach with the CFD tool ANSYS FLUENT. The heat exchanger was equipped with internal metallic fins to enhance the conductivity and even out the temperature distribution inside the PCM. Various fin configurations were evaluated and it was found that configurations with three equidistant radial fins along the 300-mm long inner pipe provided the best heat distribution in the PCM. The effect of fin lengths was investigated through a parametric study using five different fin lengths within the PCM. Using 35-mm fins in the 70-mm PCM layer yielded the most effective results, achieving a slow but close to complete melting of the PCM erythritol within a realistic combustion duration, while allowing a discharge with an extended heat release.

1. Introduction

Latent heat storage (LHS) for small-scale batch combustion is a promising concept to exploit the properties of phase change materials (PCM). For example, wood stoves rely on a batch combustion process, yielding a transient heat production with high peak heat release during combustion, often exceeding the actual needs of the end user. Typical modern wood stoves have a thermal efficiency of 70 to 80 % at nominal load and often produce more heat, especially in highly-insulated buildings, than actually required to heat up the house (Georges et al., 2013). At the end of a batch, the heat release rapidly decreases, while the need for heating may remain. A well-designed LHS system (with phase change in the range of 100-150 °C) can flatten out the heat release to the room by storing it as latent heat, before releasing it to the room again after the end of the combustion cycle. This results in a relatively stable heat release over an extended time-period. PCMs have the potential to yield a more efficient solution than current sensible heat storage solutions using e.g. soapstone. Indeed, PCM can store more heat both per mass and volume and offer a more stable heat release due to the isothermal phase change process. This is of special interest for the highly-insulated low-energy buildings and passive houses. Such LHS systems using PCM may also be designed as a retrofit to existing wood stoves. However, designing an optimal system with a suitable PCM remains challenging due to the complexity of the physical and thermal interactions between PCM, heat source and heat sink.

1.1 Objective

The objective of the current study is to design a compact and durable LHS system capable of storing a substantial part of the heat produced during combustion and to effectively release the stored heat to the room

at the end of the combustion period, for 6 to 10 hours. One of the challenges is to exploit a significant part of the heat available in the flue gas without reducing the draught in the chimney below a critical point, since this could alter the combustion process that is based on natural draught. Another challenge is to ensure melting of most of the PCM mass within a reasonable time, without overheating the PCM above its degradation temperature. The key findings and detailed results of the parametric study with varying fin length are presented.

1.2 Literature review

With a large variety of available PCMs, and a high number of properties affecting their suitability to a given application, finding the best-suited PCM is often complex. A method was developed to assist the selection process of an optimal PCM for LHS with wood stove combustion based on a one-dimensional analysis providing key indicators (Kristjansson et al., 2016). The performance of the LHS is described through the energy density, the ratio of latent to sensible heat capacity, the Biot number and an indicator of overheating risk. These indicators allow effective ranking of PCMs candidates for a given application.

Regarding geometries similar to the one selected in the present study, Al-Abidi et al. reported on a successful numerical and experimental study of a LHS system applied to a liquid desiccant air-conditioning system (Al-Abidi et al., 2013a, 2013b). The study relied on a triplex tube heat exchanger with internal and external longitudinal fins, where the PCM (with phase change in the range of 77-85 °C) was enclosed between the two concentric tubes. Results showed that the effect of fin thickness was small compared to the fin length and number of fins, which had a strong effect on the time for complete melting and solidification.

With a similar geometry in a lower temperature range, Almsater et al. (2017) presented a CFD model of a LHS in a vertical triplex tube subject to free convection and its validation through experimental results. The heat transfer fluid flowed in the outer and inner tubes, while the central space contained the PCM. Eight longitudinal fins were included to separate the PCM compartments. Water was used as PCM. It was found that the melting process duration was generally quicker compared to the freezing process due to free convection.

Various studies have investigated the opportunities for thermal energy storage associated with wood stoves. Benesch et al. (2015) developed a CFD-based methodology for the analysis and optimization of a wood stove with sensible heat storage device. The results enabled the authors to test different storage materials in solid state. The same group also developed guidelines for heat storage units based on phase change materials, still addressing wood stoves (Mandl & Obernberger, 2017). It was notably pointed out that the PCM melting temperature should not be too high to allow charging at partial combustion load. The following criteria were listed as the most important and challenging: low flammability, low thermal degradation, high heat capacity, high density, suitable melting temperature, affordability, low corrosivity and low toxicity. The advised approach in the guidelines was however a full PCM integration in the side wall(s) of the stove allowing the flue gas to flow through the PCM and to discharge heat with the assistance of free convection of room air flowing in parallel channels through the PCM.

Another study involving a wood stove manufacturer focused on the technical design and construction of a stove surrounded by flat walls filled with salt hydrates melting at 60 °C (Zielke et al., 2013). The goal was to avoid firing the stoves at partial load at night and thereby avoiding the high associated emissions, while keeping the house warm. Though the results proved positive, the solution has not yet been commercialized due to the difficulty to achieve a commercial design in line with the customers' expectations.

2. Methodology

2.1 Geometry

A coaxial cylindrical heat exchanger seemed the most promising geometry for our purpose of replacing the stovepipe above the wood stove. The PCM is located between two concentric tubes and is charged by the hot exhaust gas flowing through the vertical inner pipe from bottom to top, while the stored heat can be released later to the surroundings. In the stainless-steel coaxial cylinder, the inner tube has an outer diameter of 0.15 m, and the outer tube has an outer diameter of 0.3 m. The wall thickness for both tubes is 5 mm, leaving a 70-mm thick layer of PCM around the inner tube. While a longer coaxial cylinder may be considered in commercial applications, a length of 300 mm was kept for the simulation to represent a more acceptable total weight and to reduce the computing time.

Fins in the PCM volume, when present, are radial around the inner tube and are 3-mm thick and made of stainless steel. Though longitudinal fins have proved to enhance the melting rate in similar geometries (Al-Abidi et al., 2013b), radial fins can enable a more homogeneous melting process along the concentric pipe. Another advantage with radial fins is the opportunity to model the LHS system using 2D axisymmetry, resulting in shorter computing time than any 3D model with longitudinal fins. Previous simulations with constant wall temperature tested the effect of the number of radial fins and the separation distance in the PCM domain, from no fin to three

fins equally distributed along the 300-mm long coaxial cylinder (Soibam, 2017). Three equidistant radial fins achieved a more homogenous heat transfer across the PCM and therefore were kept for all simulations.

2.2 Material and fluid properties

The hot exhaust gas of batch wood log combustion typically being in the temperature range 100-250 °C, the PCM erythritol was considered due its melting temperature of 118 °C. The thermo-physical properties of erythritol used for the simulations are shown in

Table 1. The properties indicated for two different temperatures were modeled in ANSYS FLUENT using piece-wise linear equations. Despite its convenient thermo-physical properties, one challenge with erythritol is its low degradation temperature through irreversible decomposition from 160 °C (Kaizawa et al., 2008), while in practice its thermal properties may be altered at even lower temperatures. Supercooling of erythritol has also been reported in the literature (Höhlein et al., 2017) but was not implemented in the simulations, in view of the large temperature difference experienced in the system.

Table 1: Thermo-physical properties of erythritol (Höhlein et al., 2017), (Kaizawa et al., 2008) and (Mehling & Cabeza, 2008) used in the simulations.

Erythritol	Values
Melting temperature	118 °C
Theoretical degradation temperature	160 °C
Latent heat of solidification	339.9 kJ·kg ⁻¹
Specific heat capacity (solid, 20 °C)	1.38 kJ·(kg·K) ⁻¹
Specific heat capacity (fluid, 140 °C)	2.76 kJ·(kg·K) ⁻¹
Conductivity (solid, 20 °C)	0.733 W·(m·K) ⁻¹
Conductivity (fluid, 140 °C)	0.326 W·(m·K) ⁻¹
Density (solid, 20 °C)	1480 kg·m ⁻³
Density (fluid, 140 °C)	1300 kg·m ⁻³

Table 2: Thermo-physical properties of exhaust gas used in the simulations.

Hot exhaust gas	Values
Composition	7 % CO ₂ , 13 % O ₂ , 20 % H ₂ O and 60 % N ₂
Temperature	225 °C
Density	0.72 kg·m ⁻³
Specific heat capacity	1.155 kJ·(kg·K) ⁻¹
Viscosity	2.46·10 ⁻⁵ kg·(m·s) ⁻¹
Conductivity (pure gas)	0.035 W·(m·K) ⁻¹
Conductivity (with heat transfer enhancement)	2.45 W·(m·K) ⁻¹

The thermo-physical properties of the hot exhaust gas shown in Table 2 were calculated at 225 °C using GASEQ based on a composition representative of the exhaust gas flowing out of wood stoves. The first simulations showed that the heat transfer rate from the hot exhaust gas through the inner tube towards the PCM was insufficient without using any heat transfer enhancement method (Soibam, 2017). Therefore, eight longitudinal fins were added on the hot exhaust gas side to enhance the heat transfer towards the inner tube. In the simulations, the fins are represented through the calculated volume-averaged effective heat conductivity of the hot exhaust gas of 2.45 W·(m·K)⁻¹ instead of 0.035 W·(m·K)⁻¹ for the pure hot gas.

2.3 Computational models and conditions in ANSYS FLUENT

The 2D-axisymmetrical geometry was modelled in ANSYS FLUENT 17.2 using gravitational acceleration. A fine mesh was used, encompassing ca. 65,000 cells with a refined mesh in the near-wall regions. The temperature range for the phase change was set to 3 K, centered on the melting temperature, since it enabled sufficient calculation stability, which narrower temperature ranges did not. It should be noted that the temperature range is to some extent dependent on the mushy zone constant (10⁵ was used here), as shown by Kheirabadi & Groulx (2015). The solution method relied on the PRESTO scheme for the pressure correction equation and the Semi-Implicit Pressure-Linked Equation (SIMPLE) algorithm for the pressure-velocity coupling. Momentum, turbulent kinetic and energy equations were solved using a first-order discretization. To enable converged solutions, the relaxation factors were set to 0.1 for liquid fraction, 0.3 for pressure and momentum, 0.8 for density, turbulent kinetic energy and turbulent dissipation rate, 0.9 for energy and 1 for body forces.

For the charging process (melting), the inlet boundary in the gas domain was set to a velocity-inlet with a value of 1 m·s⁻¹, and a constant inlet temperature of 498 K to simulate the hot exhaust gas flowing through the stovepipe. The outlet boundary in the gas domain was set as an outlet-vent. The outer pipe wall towards the room was set to have mixed thermal conditions, i.e. heat is transferred to the outside due to convection and radiation. The heat transfer coefficient for convection was set to 25 W·m⁻²·K⁻¹ with a free-stream temperature of 25 °C. The coefficient was chosen higher than for regular free convection in order to represent the effect of the convective air flows originating from the hot wood stove underneath the stovepipe. For the radiation, the wall emissivity was set to 0.85. The bottom and top walls of the PCM domain were defined as adiabatic walls. The whole LHS system temperature was initially set to 25 °C.

For the discharging process (solidification), the inlet and outlet boundaries of the hot gas domain were represented as adiabatic walls, considering a virtual valve blocking the gas flow in the stovepipe once combustion is over. In reality, the gas flow would not be fully blocked, due to the need to evacuate the remaining exhaust gas from the charcoal burnout phase. This simplification minimized the heat losses through the inner pipe and especially eased the comparison between the different cases. As initial conditions, the hot gas domain was patched at 100 °C, which is a relatively high temperature, though still below the PCM's melting temperature. In the PCM domain, the fins and inner pipe were patched with a temperature of 122 °C. Two different initial conditions were studied in the PCM domain: (1) starting from a constant and homogeneous temperature of 122 °C, which is above the PCM melting temperature, and (2) starting from the liquid fraction and temperature fields as established after 6 hours of melting at the above-mentioned conditions, to mimic a dynamic case with sudden change of external conditions. For the first initial condition, the outer pipe temperature was set to 116 °C, which is an average temperature obtained by the end of the above-mentioned melting processes.

Five fin lengths, for fins attached to the inner pipe in the PCM domain, were studied under the described conditions. The five lengths corresponded to 0 mm (no fins), 17.5 mm (one quarter of the PCM thickness), 35 mm (half-way through the PCM volume), 52.5 mm (three quarters of the PCM thickness) and 70 mm (fin joining the inner pipe to the outer pipe). The parametric study enabled to understand the fin length's effects on melting and solidification processes and to determine the most relevant fin length for the application with wood stoves.

3. Results and discussion

3.1 Liquid fraction

Figure 1 shows the effect of the fin length on the mass-averaged liquid fraction for 6 h of charging followed by a discharge. A 6-hour duration corresponds to a realistic average combustion duration when using several batches in wood stoves. After that duration, the boundary conditions were changed in the inner pipe to trigger the discharge. Simulations running charging only (melting) revealed that with the 70-mm fins, 11.5 hours were needed to fully melt the PCM, and none of the other tested fin configurations reached full melting. In Figure 1, the liquid fraction with the 70-mm fins lies below the other configurations with fins until 6 h into the charging process. The configuration with no fins hardly reached a liquid fraction of 0.6. The fastest melting rate occurred for the configuration with 17.5-mm fins due to an effective combination of conduction into the warmest part of the PCM and only a small restriction of movement for the convective transport to enhance the heat exchange through the PCM mass. The highest liquid fraction in 6 h was achieved with 35-mm fins (0.945).

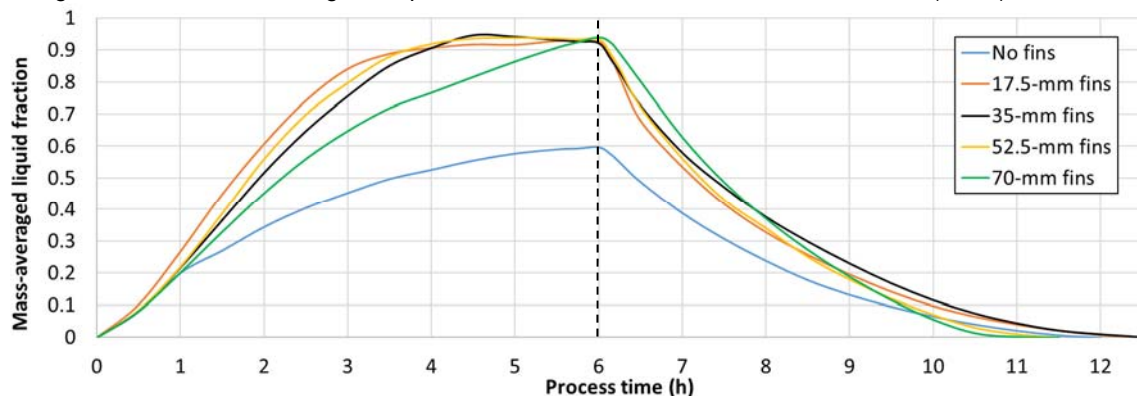


Figure 1: Effect of fin length on liquid fraction for 6 h of charging (melting) followed by a discharge (solidification).

As shown in Figure 1, using 35-mm and 52.5-mm fins, the liquid fraction reached a top within 4.5 to 5 h of charging. However, as the heat transfer from the hot exhaust gas continues, the liquid fraction slightly decreased instead of following the expected increasing trend. This effect was due to the free convection effects, transporting the hotter melted PCM through buoyancy to the top, while the cooler melted PCM was transported to the bottom, eventually cooling down the lower part of the PCM block below the melting temperature. The effect was amplified by the continuous heat exchange between the melted PCM and the outer pipe, which released heat by radiation and convection to the room, having an ambient temperature.

During the discharging process, the configuration with 70-mm fins first kept a higher liquid fraction and then yielded a significantly higher rate of solidification than all the other cases. With 70-mm fins, the PCM was fully solidified after 4.5 h, followed by the case with the 52.5-mm fins, after 5 h.

Figure 2 shows the liquid fraction in the 2D axisymmetric model after 1 h of charging, for the tested fin lengths. For all configurations with fins, the effects of buoyancy, yielding free convection, were visible through the melted PCM accumulating under the fins. After 1 h of charging, the melted PCM reached a sufficient volume to pass beyond some of the fins for the cases with 17.5-mm and 35-mm fins. Without fins, the effects of free convection led to a noticeably higher melted fraction in the upper part of the PCM domain, close to the inner pipe. In comparison, the melted fraction in the cases with fins was more homogeneously distributed.

A key observation is the sharp mushy zone during the melting process, corresponding to the volume where the PCM is neither fully liquid nor solid. In comparison, the mushy zone appeared significantly broader during the solidification process. This is due to the convective transport playing a major role in the melting process and yielding shear strain on the mushy zone, while the solidification process is primarily conduction-driven with almost no convective transport of melted PCM (Fleischer, 2015).

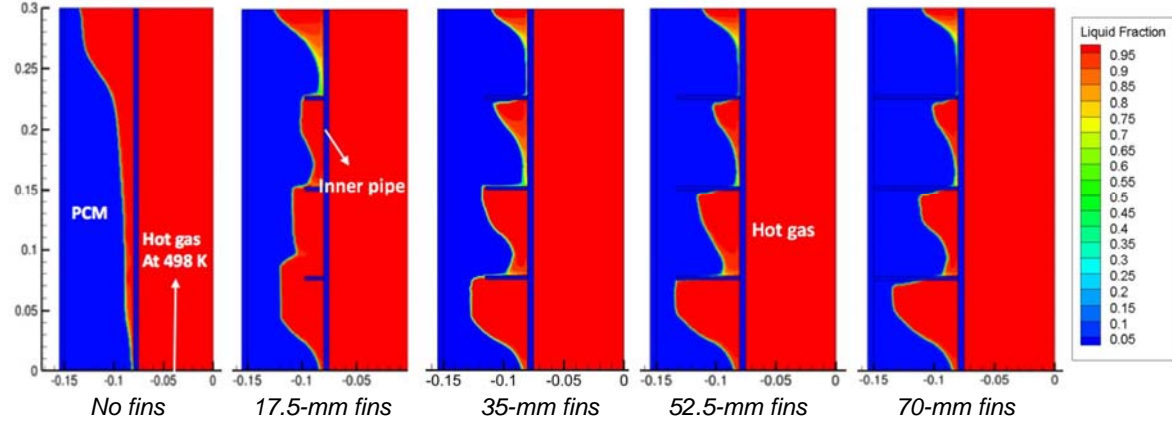


Figure 2: Effect of fin length on liquid fraction, 1 h after the start of melting process.

3.2 Heat transfer to the surrounding

Figure 3 shows the effect of fin length on the heat transferred by radiation and convection from the outer pipe to the room for 6 h of charging followed by a discharge. For the case with 70-mm fins, the amount of heat transferred from the outer pipe wall became larger than for the other cases after 5 h. The 70-mm fins, however, contributed to the heat loss to the room before it was needed, with up to 100 W more than with 35-mm fins at times. A similar behavior was found with 52.5-mm fins. With 70-mm fins, the mass-averaged PCM temperature rose beyond the melting point after 5 h, eventually elevating local PCM temperature up to 166 °C, which is beyond erythritol's critical degradation temperature. The cases with 35-mm fins and no fins kept the local PCM temperature under 148 °C, while up to 154 °C was reached locally with 17.5-mm and 52.5-mm fins.

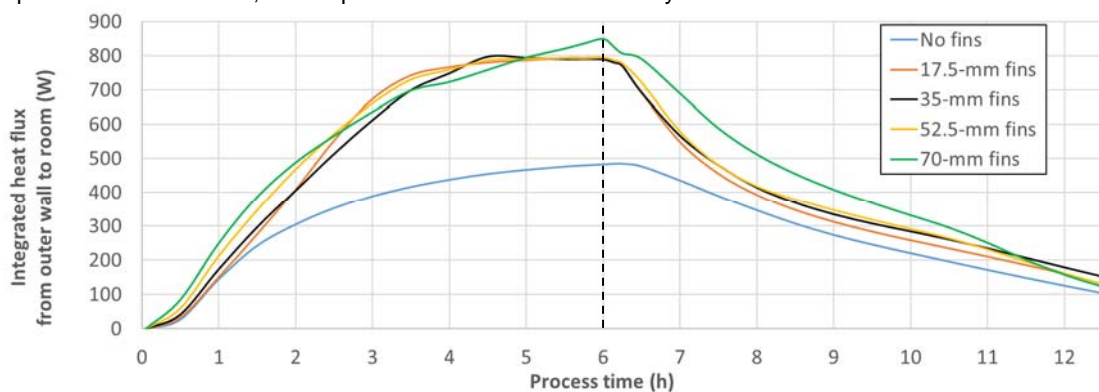


Figure 3: Effect of fin length on the heat transferred from the outer pipe to the room for 6 h of charging (melting) followed by a discharge (solidification).

For the configurations with 17.5-mm, 35-mm and 52.5-mm fins, a thermal balance was almost reached after 4.5 hours, when the amount of transferred heat first flattened and eventually slightly decreased. The decrease was most likely due to a local re-solidification phenomenon which occurred in the lower part of the PCM domain, as described previously.

The sudden change in supplied heat after 6 h marked the start of the discharging process. The heat loss to the inner pipe was minimal due to the blockage of the gas flow in the inner pipe. The lowest heat release was associated with the configuration with no fins, though the total heat that can be released is naturally lower than for the other cases since a lower fraction of PCM was melted after 6 h. The configuration with 70-mm fins provided the highest heat release for ca. 5.5 h, until the heat release with 35-mm fins became higher.

It should be noted that the heat transfer coefficient of $25 \text{ W}\cdot\text{m}^{-2}\cdot\text{K}^{-1}$ used for convection for the outer pipe wall towards the room was rather high. A lower coefficient, closer to a regular free convection coefficient in the range of $5\text{-}10 \text{ W}\cdot\text{m}^{-2}\cdot\text{K}^{-1}$, may be more realistic and would yield a lower solidification rate by limiting the heat loss to the room. A further improvement would be to allow the convection coefficient to change with time, to include the transient influence of the significant convective air flow around the stove. Due to the generally large thermal inertia of wood stoves, convection flows around them typically increase to a maximum value during the combustion phase and slowly decrease as they cool down in the absence of combustion.

4. Conclusions

A passive LHS system designed as a coaxial cylinder acting as a stovepipe located at the top of a wood stove was simulated by transient 2D axisymmetric CFD modelling with ANSYS FLUENT. The heat exchanger was equipped with internal radial metallic fins to enhance the conductivity and even-out the temperature distribution inside the PCM. Various fin configurations were evaluated through numerical simulations.

The configuration with 35-mm fins provided the best trade-off for our application. With 35-mm fins, the PCM storage could be loaded relatively fast (i.e. 4.5 h), while still yielding a long heat release over 6-10 h. The local PCM temperature was kept under $148 \text{ }^\circ\text{C}$, whereas the other tested configurations with fins reached maximum local PCM temperature closer to or beyond erythritol's degradation temperature of $160 \text{ }^\circ\text{C}$.

Erythritol's degradation temperature is possibly too low for batch combustion applications displaying a high transient behavior and potentially higher maximum temperatures in the hot exhaust gas than tested here. The critical degradation temperature might also be reached in cases where several consecutive batches are fired. Further investigations could be conducted with more advanced fin configurations, such as non-uniform distance between fins and more complex fin shapes, for example. Experimental validations would also be of interest.

Acknowledgements

The study was carried out through the research project PCM-Eff - Novel phase change material solutions for efficient thermal energy storage - supported by SINTEF Energy Research and the Research Council of Norway.

References

- Al-Abidi, A. A., Mat, S., Sopian, K., Sulaiman, M. Y., Mohammad, A. T., 2013a, Internal and external fin heat transfer enhancement technique for latent heat thermal energy storage in triplex tube heat exchangers. *Applied Thermal Engineering*, 53(1), 147-156.
- Al-Abidi, A. A., Mat, S., Sopian, K., Sulaiman, M. Y., Mohammad, A. T., 2013b, Numerical study of PCM solidification in a triplex tube heat exchanger with internal and external fins. *International Journal of Heat and Mass Transfer*, 61, 684-695.
- Almsater, S., Alemu, A., Saman, W., Bruno, F., 2017, Development and experimental validation of a CFD model for PCM in a vertical triplex tube heat exchanger. *Applied Thermal Engineering*, 116, 344-354.
- Benesch, C., Blank, M., Scharler, R., Kössl, M., Obernberger, I., 2015, Transient CFD Simulation of Wood Log Stoves with Heat Storage Devices. Presented at the 21st European Biomass Conference and Exhibition.
- Fleischer, A. S., 2015, *Thermal energy storage using phase change materials: fundamentals and applications*: Springer.
- Georges, L., Skreiberg, Ø., Novakovic, V., 2013, On the proper integration of wood stoves in passive houses: Investigation using detailed dynamic simulations. *Energy and Buildings*, 59(Supplement C), 203-213.
- Höhlein, S., König-Haagen, A., Brüggemann, D., 2017, Thermophysical Characterization of $\text{MgCl}_2\cdot 6\text{H}_2\text{O}$, xylitol and erythritol as phase change materials for latent heat thermal energy storage. *Materials*, 10(4), 444.
- Kaizawa, A., Maruoka, N., Kawai, A., Kamano, H., Jozuka, T., Senda, T., Akiyama, T., 2008, Thermophysical and heat transfer properties of phase change material candidate for waste heat transportation system. *Heat and Mass Transfer*, 44(7), 763-769.
- Kheirabadi, A. C., Groulx, D., 2015, Simulating phase change heat transfer using Comsol and Fluent: Effect of the mushy-zone constant. *Computational Thermal Science*, 7(5-6), 427-440.
- Kristjansson, K., Næss, E., Skreiberg, Ø., 2016, Dampening of wood batch combustion heat release using a phase change material heat storage: Material selection and heat storage property optimization. *Energy*, 115, Part 1, 378-385.
- Mandl, C., Obernberger, I., 2017, *Guidelines for heat storage units based on Phase Change Materials (PCM)*.
- Mehling, H., Cabeza, L. F., 2008, *Heat and cold storage with PCM*: Springer, Berlin, Heidelberg.

Soibam, J., 2017, Numerical Investigaton of a Phase Change Material Heat Exchanger for Small-Scale Combustion Appliances. (Master Degree), NTNU, Trondheim, Norway.

Zielke, U., Bjerrum, M., Nørgaard, T., 2013, Slow Heat Release - Brændeovn med salhydratvarmelager - Miljøprojekt nr. 1438.